Figures

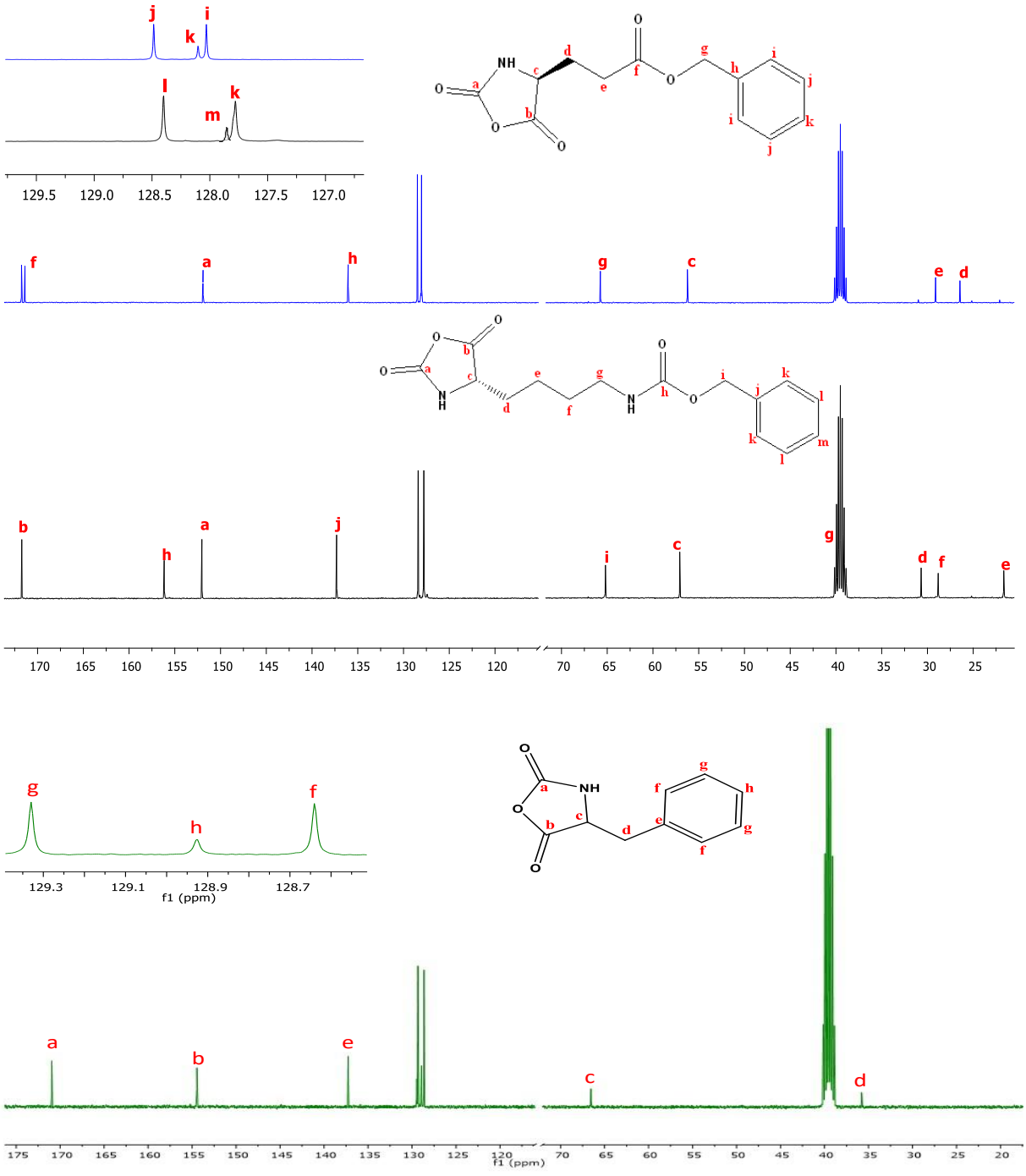

Figure S1: ^{13}C NMR of Glu (OBzl)-NCA [blue]; Lys(Z)-NCA [black] and Phe-NCA [green].

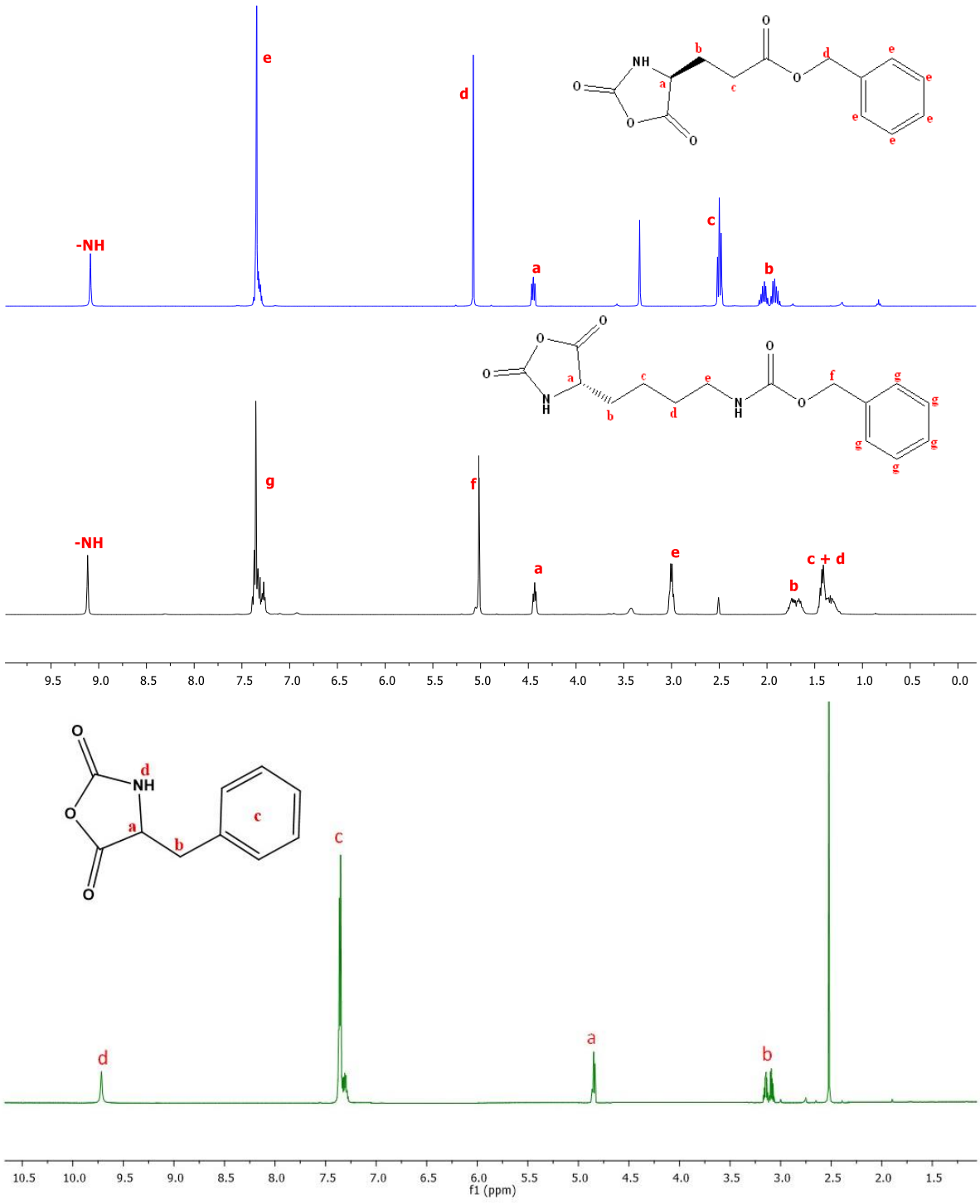

Figure S2: ^{1}H NMR of Glu (OBzl)-NCA [blue]; Lys(Z)-NCA [black] and Phe-NCA [green].

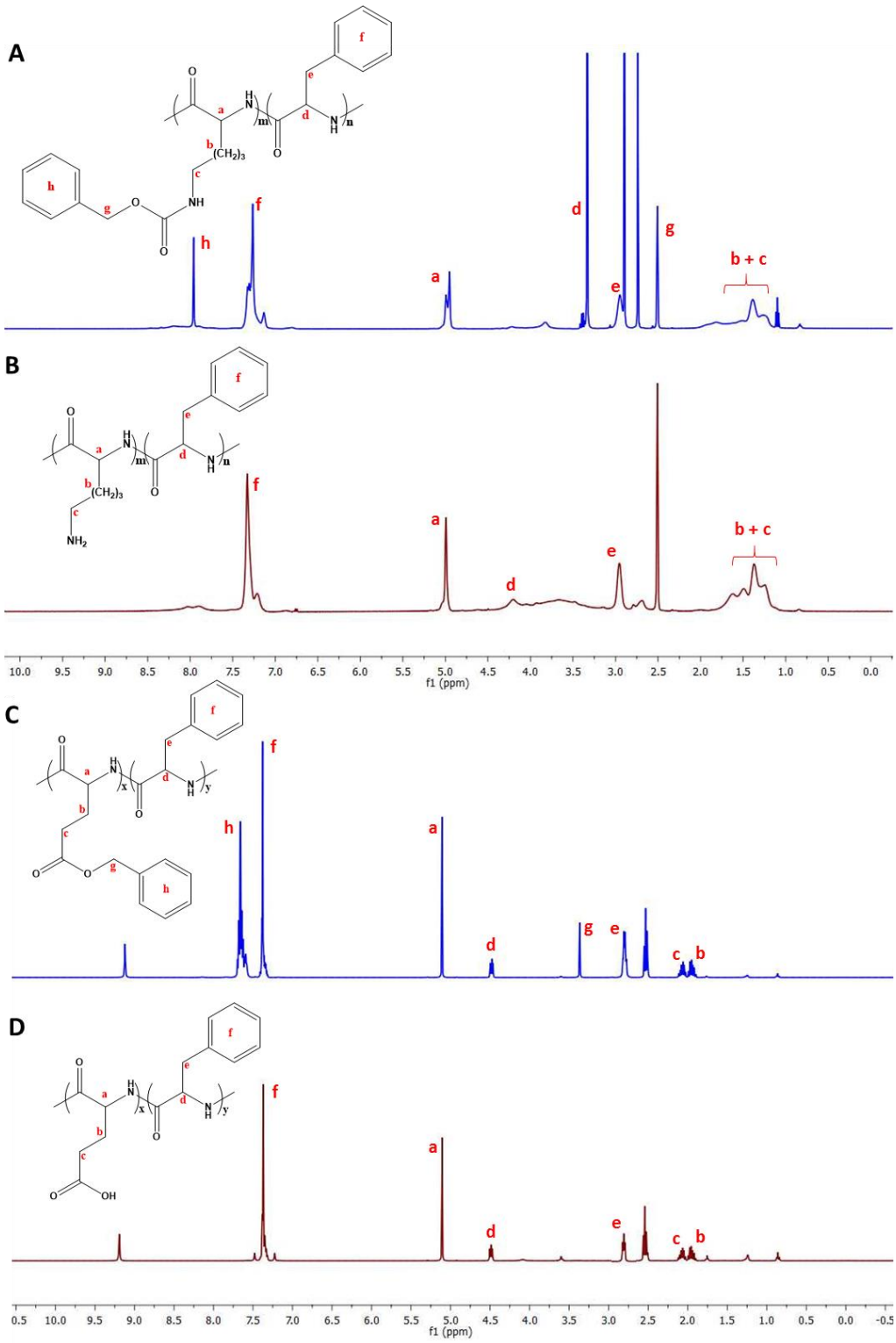

Figure S3: ^{1}H NMR of synthesized polymers A. PLL-PPA (poly L lysine-b-poly phenylalanine) protected; B. PLL-PPA deprotected; C. PGA-PPA (poly glutamic acid-b-poly phenylalanine) protected and D. PGA-PPA deprotected.

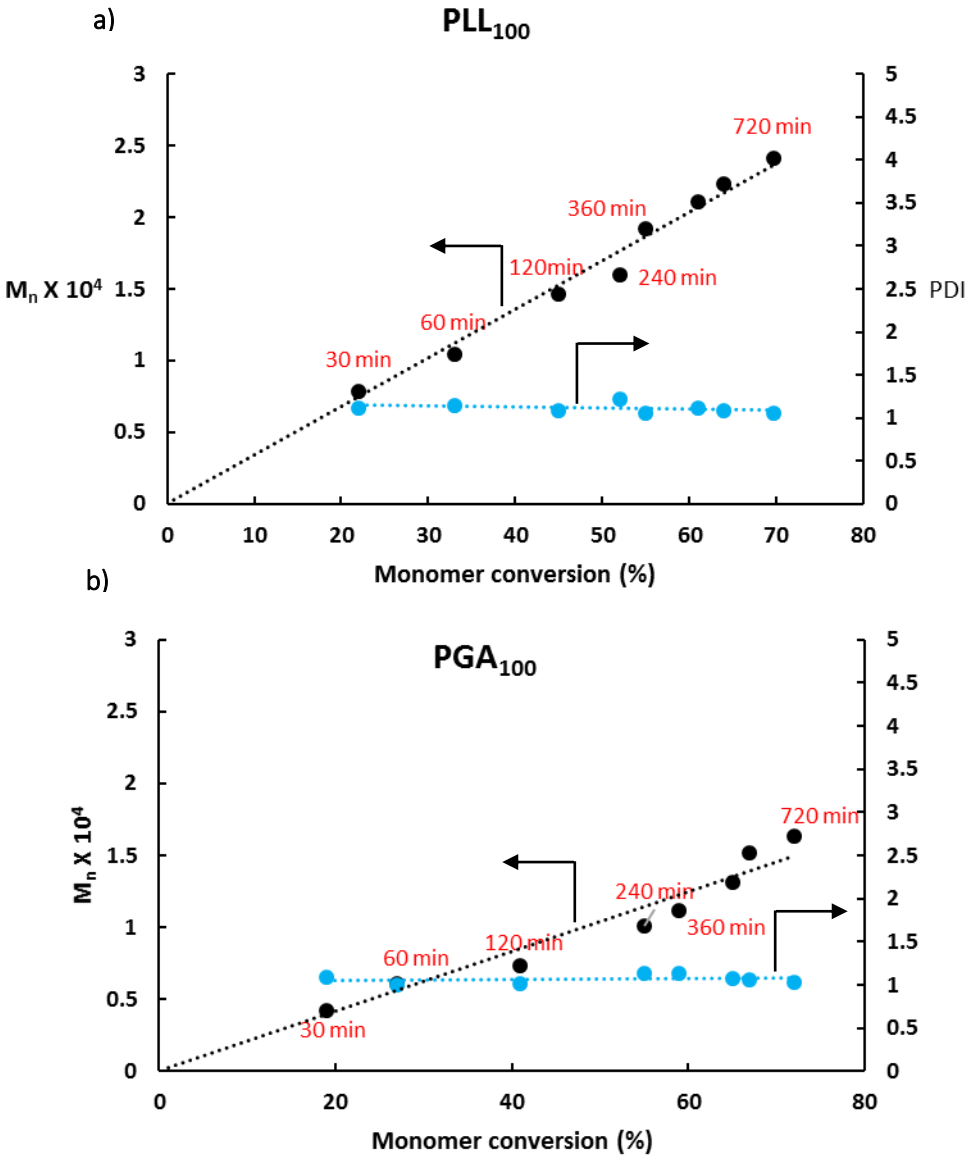

Figure S4: Molecular weight (M_n) and the PDI as a function of monomer conversion showing the controllability of the polymerization reaction; **a.** PLL block and **b.** PGA block

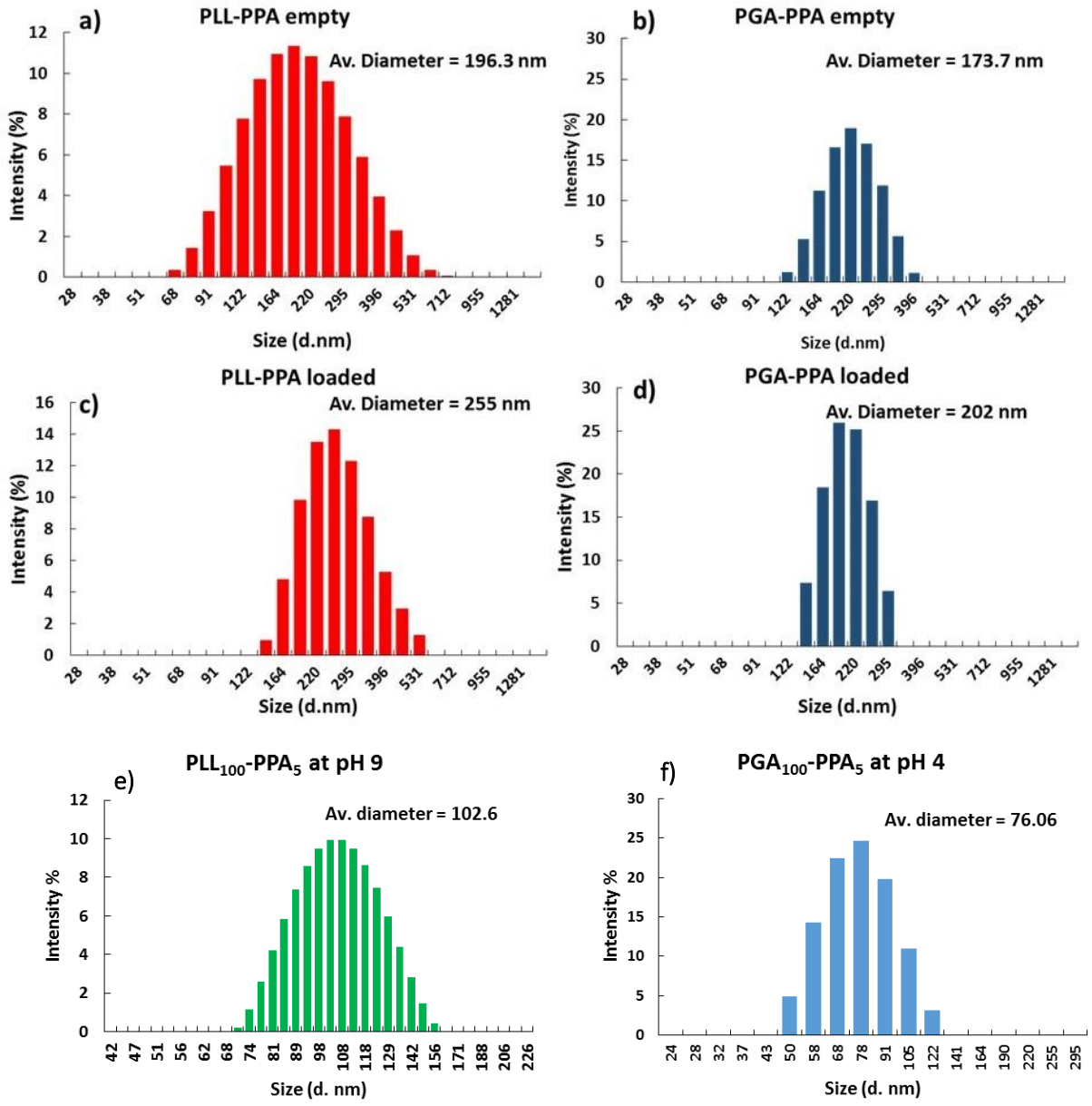

Figure S5: Dynamic Light Scattering (DLS) results (a) and (c) show PLL-PPA micelles before and after curcumin loading; (b) and (d) show PGA-PPA micelles before and after loading of amphotericin B; (e) and (f) showing the change in hydrodynamic diameter of PLL_{100}-PPA_5 and PGA_{100}-PPA_5 at pH 9.0 and 4.0 respectively.

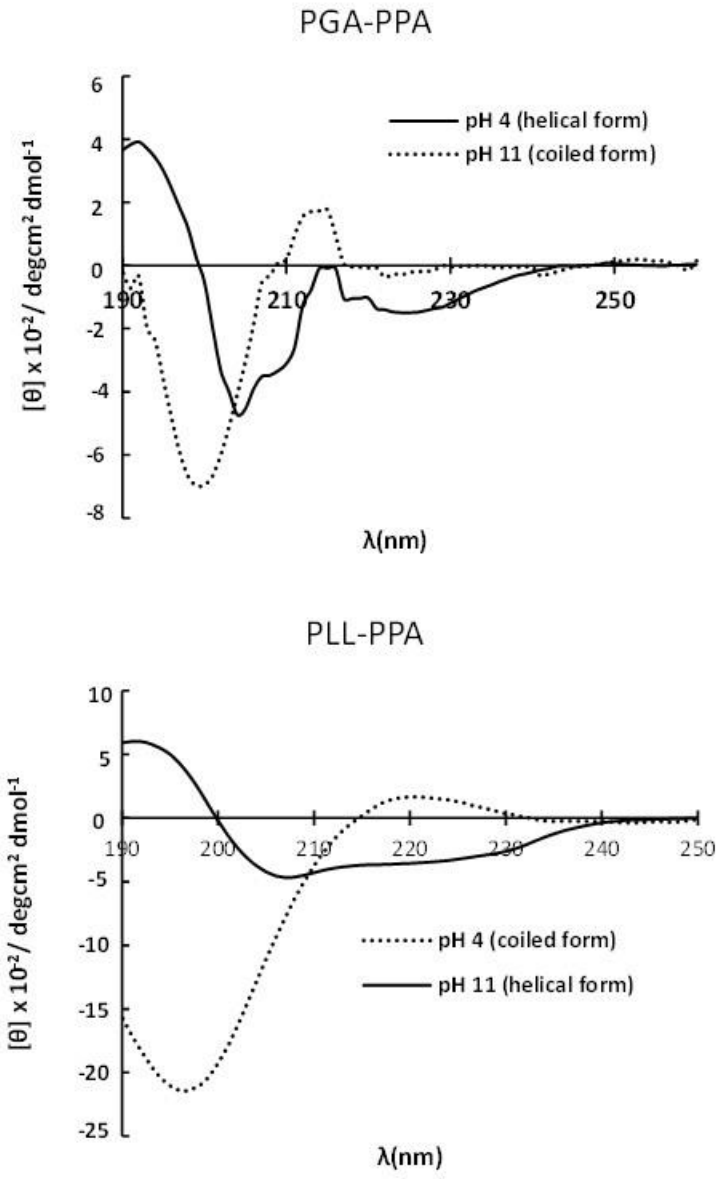

Figure S6: CD spectra of PGA-PPA (top) and PLL-PPA (bottom) at pH showing their respective transitions from random coil to α-helix at change in pH.

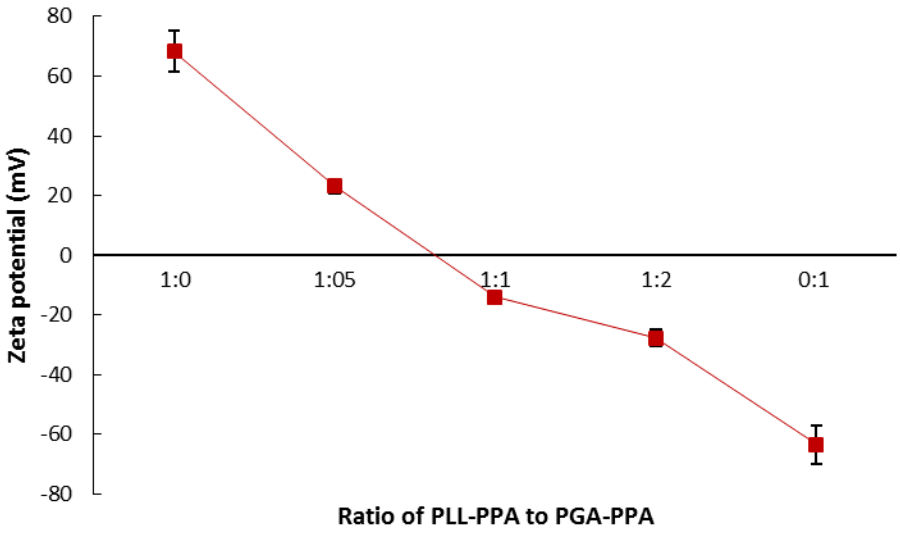

Figure S7: Variations in zeta potential of various ratios of PLL-PPA: PGA-PPA micelles.

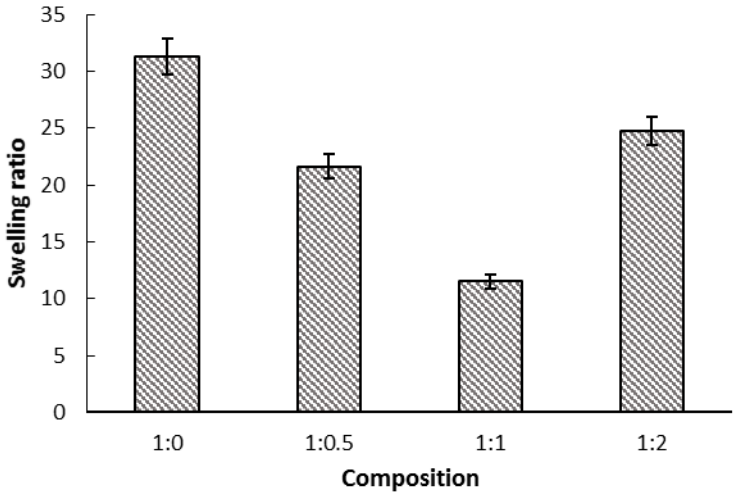

Figure S8: The equilibrium swelling ratios of the composites with varying ratios of PLL-PPA: PGA-PPA. (n=3)